RSC Advances

PAPER

View Article Online
View Journal | View Issue

Cite this: *RSC Adv.*, 2024, **14**, 5309

Bimetallic nanoparticle production using *Cannabis sativa* and *Vitis vinifera* waste extracts

Jana Michailidu, * Anna Miškovská, Irena Jarošová, Alena Čejková and Olga Mat'átková

The utilization of waste materials for the synthesis of nanoparticles has gained significant attention due to its potential for waste valorization and contribution to circular economy. In this study, bimetallic nanoparticles were produced using extracts derived from *Cannabis sativa* and *Vitis vinifera* waste, focusing on their green synthesis and antimicrobial activity against Gram-negative bacteria, specifically several strains of *Pseudomonas aeruginosa*. The *Vitis vinifera* canes and post-extraction waste from *Cannabis sativa* were processed using an ethanol extraction method. The extract was then mixed with silver nitrate and tetrachloroauric acid solution at different reagent ratios to optimize the synthesis process. The resulting bimetallic nanoparticles (AgAuNPs) were characterized using UV-vis spectrophotometry, transmission electron microscopy, atomic absorption spectrometry, X-ray diffraction, X-ray photoelectron spectroscopy and Fourier transform infrared spectroscopy. The antimicrobial activity of the biosynthesized AgAuNPs was evaluated against various strains of *Pseudomonas aeruginosa*. The minimal inhibitory concentration (MIC) was determined using a microcultivation device, and the minimal bactericidal concentration (MBC) was determined through subsequent solid medium cultivation. Additionally, the minimal biofilm inhibitory concentration (MBIC) was assessed using a polystyrene microtiter plate as biofilm carrier and measured through an assay determining the metabolic activity of biofilm cells. The results demonstrated successful synthesis of bimetallic nanoparticles using the extracts from *Cannabis sativa* and *Vitis vinifera* waste. The AgAuNPs exhibited significant antimicrobial activity against the tested *Pseudomonas aeruginosa* strains, inhibiting their growth and biofilm formation. These findings highlight the potential of waste valorization and circular economy in nanoparticle production and their application as effective antimicrobial agents. This study contributes to the growing field of sustainable nanotechnology and provides insights into the utilization of plant waste extracts for the synthesis of bimetallic nanoparticles with antimicrobial properties. The findings support the development of eco-friendly and cost-effective approaches for nanoparticle production while addressing the challenges of waste management and combating microbial infections.

Received 19th October 2023
Accepted 30th January 2024

DOI: 10.1039/d3ra07134k

rsc.li/rsc-advances

Introduction

In the era of sustainability and waste valorization, the exploration of innovative approaches for the production of valuable materials from waste streams has gained tremendous significance. Nanotechnology, with its diverse applications and unique properties, provides a promising avenue for waste valorization and the transition towards circular economy. One intriguing approach involves the synthesis of bimetallic nanoparticles using waste extracts derived from *Cannabis sativa* and *Vitis vinifera*, two plants known for their versatile applications in medicine, industry, and agriculture.[1]

The concept of circular economy emphasizes the efficient utilization of waste materials to create new value-added products, thereby minimizing waste generation and reducing environmental impact. *Cannabis sativa* and *Vitis vinifera* cultivation and industrial processing generate substantial amounts of waste. Traditionally, this waste has been discarded, composted or burned, leading to economic losses and environmental concerns. However, recent research has unveiled the presence of bioactive compounds in these waste materials, such as flavonoids, terpenes, and phenolic compounds, which possess inherent reducing and stabilizing properties suitable for nanoparticle synthesis. This approach is also highly cost-effective, as it transforms otherwise discarded materials into valuable nanoparticles, thus providing a dual benefit of waste reduction and resource creation. These plant-derived nanoparticles are characterized by reduced toxicity and possess an inherent biocompatibility compared to their chemically synthesized counterparts. Furthermore, the bioactive compounds in these extracts, such as flavonoids and phenolic compounds, impart enhanced stability and functionality to the

UCT Prague, Technická 5, 166 28 Prague 6, Dejvice, Czech Republic

nanoparticles, adding value to their application in various domains.[2–5]

Nanoparticles, especially bimetallic nanoparticles, have emerged as promising nanomaterials with unique physicochemical properties and multifaceted applications. The combination of two different metals in bimetallic nanoparticles can lead to synergistic effects, resulting in enhanced catalytic and antimicrobial activity, improved electrical conductivity, and tailored optical properties. These attributes make bimetallic nanoparticles desirable for applications as sensors, or in energy storage, catalysis, and environmental remediation.[6,7]

In addition to their remarkable properties, bimetallic nanoparticles have demonstrated significant antimicrobial activity against a broad range of microorganisms, including Gram-negative bacteria, such as *Escherichia coli* and *Pseudomonas aeruginosa*. These are notorious for their high resistance to antibiotics and pose a serious threat to public health. The antimicrobial properties of bimetallic nanoparticles stem from their unique surface characteristics, which enable efficient interaction with bacterial cell membranes and subsequent disruption of vital cellular processes. The small size and large surface area of nanoparticles facilitate enhanced contact with bacterial cells, leading to membrane damage, disruption of metabolic pathways, and generation of reactive oxygen species (ROS) that contribute to bacterial inactivation.[8–10]

By capitalizing on the waste valorization potential of *Cannabis sativa* and *Vitis vinifera* extracts, along with the synthesis of bimetallic nanoparticles, this study aimed to achieve a dual goal: sustainable waste management and the production of antimicrobial nanomaterials. Specifically, we investigated the green synthesis methodologies for obtaining nanoparticles from the waste extracts of these plant species, characterizing their physicochemical properties using techniques such as atomic absorption spectrometry (AAS), X-ray diffraction (XRD), X-ray photoelectron spectroscopy (XPS), transmission electron microscopy (TEM), and Fourier transform infrared spectroscopy (FTIR), and evaluating their antimicrobial activity against Gram-negative bacterium *Pseudomonas aeruginosa* strains (see Fig. 1).

This research holds significant promise for the integration of waste valorization, circular economy principles, and in the development of sustainable antimicrobial solutions. By harnessing the untapped potential of *Cannabis sativa* and *Vitis vinifera* waste extracts, we can simultaneously address environmental concerns, create value from waste, and contribute to the fight against antibiotic resistance by preparing a new disinfectant alternative that would have the potential to be used in the hospital environment to eliminate nosocomial pathogens.

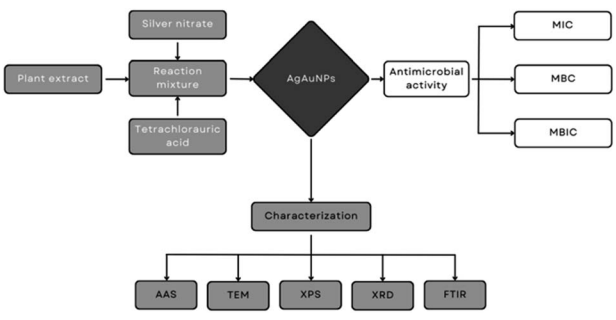

Fig. 1 Flowchart summarizing the contents of the study, showing the bimetallic nanoparticle synthesis method and the subsequent physico-chemical characterization as well as antimicrobial activity experiments.

Experimental

Preparation of plant extract

The materials utilized for biosynthesis consisted of dried *Vitis vinifera* canes which were collected during dormancy period and waste material after *Cannabis sativa* cannabinoid extraction, both located from sources in the Czech Republic. Additional materials included silver nitrate and tetrachlorauric acid obtained from Sigma Aldrich, ethanol (40%), and distilled water, ultrapure water.

Preparation of plant extract

To extract the desired compounds, a modified extraction method based on Rollová *et al.* was employed.[11] The *Vitis vinifera* canes and *Cannabis sativa* waste were homogenized using a blade blender, and 150 g of the homogenized material was mixed with 600 mL of a 40% ethanol solution. This mixture underwent maceration for 24 hours in room temperature and was subsequently filtered through an 8 μm filter paper, followed by a 0.2 μm filter paper to remove impurities. The resulting extract was stored in dark at 7 °C for further use in the synthesis process.

Green synthesis of bimetallic nanoparticles

The green synthesis method, modified according to AbdelHamid *et al.*,[12] was employed for the production of bimetallic nanoparticles (AgAuNPs) using the ethanolic extract of *Vitis vinifera*/*Cannabis sativa*, tetrachloroauric acid and silver nitrate solution. Several reagent ratios were tested during the synthesis process. Initially, 10% v/v of *Vitis vinifera*/*Cannabis sativa* extract was added to tetrachloroauric acid and silver nitrate solutions of varying concentrations (1 : 1, 2 : 1, 3 : 1, 2 : 2 mM). The ratios were selected by an analysis of the constituent substances present in the extract and the concentrations of metal precursors documented in existing literature. This investigation involved a systematic exploration of a range of ratios, and the final choice was informed by the outcomes that exhibited the highest level of efficacy and alignment with the established scientific knowledge. The reaction mixture was allowed to react for 48 hours, and the resulting dispersion of AgAuNPs was characterized using UV-vis spectrophotometry. Based on these pilot experiments, the final reagent ratios with the preferable UV-vis characteristics for the antimicrobial testing stock dispersions were determined as 10% v/v of *Vitis vinifera* extract with a 2 : 2 mM solution of tetrachloroauric acid and silver nitrate, and 10% v/v of *Cannabis sativa* extract with a 1 : 1 mM solution of tetrachloroauric acid and silver nitrate.

Nanoparticle characterization

For the characterization of synthesized nanoparticles, analyses were performed including transmission electron microscopy (TEM), atomic absorption spectrometry (AAS), X-ray diffraction (XRD), X-ray photoelectron spectroscopy (XPS) and Fourier transform infrared spectroscopy (FTIR). In the TEM method, the nanoparticles were analysed as dispersion including the extract, while the AAS method utilized the supernatant obtained by centrifuging (49.054 g for 30 min) the nanoparticles suspended in extract. The nanoparticles were centrifuged, resuspended in ultrapure water, and subsequently lyophilized for the XRD and XPS methods. TEM characterization was conducted using the EFTEM Jeol 2200 FS instrument, followed by image analysis using ImageJ software. AAS characterization was performed using the AGILENT 280 FS AA instrument, while XRD characterization utilized the PANalytical X'Pert PRO diffractometer with CuKα radiation. The elemental composition of the nanoparticle surface was investigated using XPS on the ESCA ProbeP instrument. The molecular structure of the stabilizing layer on the nanoparticles was analyzed using FTIR on the Nicolet 6700 instrument.

Microbial strains and growth media

The study utilized five strains of *Pseudomonas aeruginosa*: PAO1, ATCC 10145, ATCC 15442 from the American Type Culture Collection and DBM 3081, and DBM 3777 which were obtained from the Collection of Microorganisms of the Department of Biochemistry and Microbiology, UCT Prague. Glycerol cryopreserves of these strains were stored at −70 °C. These strains represent a wide range of phenotypes from a soil isolate to the most researched clinical isolate, PAO1.

Prior to each experiment, all *P. aeruginosa* strains were precultivated in a Luria–Bertani (LB) liquid medium at 37 °C for 24 hours to achieve the exponential growth phase. The cultivation was carried out in Erlenmeyer flasks with a volume of 100 mL and agitation at 150 rpm.

Evaluation of minimal inhibitory concentration (MIC)

To assess the antimicrobial effects of the biosynthesized silver nanoparticles (AgAuNPs) against planktonic cells, a microcultivation device (Bioscreen C, Finland) and the microdilution method, following the approach of Sharma *et al.*, were employed.[13] The *P. aeruginosa* cells were cultivated in a microtiter plate for 24 hours, with different percentages (v/v) of AgAuNPs added to each well. The experiment was conducted in 10 parallels in 3 independent repetitions. The wells contained LB medium (160 μL), inoculum (30 μL, OD_{600} = 0.1), and varying ratios of phosphate buffer saline solution and AgAuNPs (0.31, 0.63, 1.25, 1.88, 2.50, and 3.13% v/v). Control parallels consisted of LB medium, inoculum, and phosphate buffer saline solution. The growth curves obtained from the microcultivation device data were used to determine the minimal inhibitory concentration (MIC_{80}). MIC_{80} represents the lowest concentration of the antimicrobial agent that resulted in 80% inhibition of growth compared to the control after overnight cultivation.[14] The specific MIC value was derived from three independent replicates, all yielding the same result within the range of studied concentrations.

Evaluation of minimal bactericidal concentration (MBC)

The bactericidal effect of the biosynthesized nanoparticles was assessed by performing subsequent solid medium cultivations using LB agar plates. Planktonic cells from the previous cultivation in the presence of nanoparticles were transferred to the agar plates. The *P. aeruginosa* cells were cultivated for 24 hours in a microtiter plate with different percentages (v/v) of AgAuNPs derived from their respective MICs (1× MIC, 2× MIC, 5× MIC). The experiment was conducted in 10 parallels in 3 independent repetitions, and control parallels contained LB medium, inoculum (30 μL, OD_{600} = 0.1), and phosphate buffer saline solution. A total of 10 μL of cell suspension representing each nanoparticle concentration and the control were inoculated onto the LB agar plate and cultivated for an additional 24 hours. The minimal bactericidal concentration (MBC) was determined as the concentration that resulted in the growth of fewer than five colonies (indicating >99% killing) through the evaluation of growth on solid medium, following the method of Rahal and Simberkoff.[15] The MBC determination was based on three independent replicates, each consistently resulting in the same outcome across the spectrum of investigated concentrations. Statistical analysis was performed using Statistica 13.5 (StatSoft, TIBCO Software, 241 United States). One-way ANOVA was performed, followed by Tukey's multiple comparisons post hoc test for the measurement of significant differences ($P < 0.05$) among the treatments.

Evaluation of minimal biofilm inhibitory concentration (MBIC)

For the assessment of minimal biofilm inhibitory concentration (MBIC), cultivation was carried out in polystyrene 96-well microtiter plates. The *P. aeruginosa* cells were cultivated for 24 hours in the presence of different percentages (v/v) of AgAuNPs derived from their respective MICs, ranging from 0% v/v to 3× MIC. Each well contained an inoculum (210 μL, OD_{600} = 0.8) with varying ratios of phosphate buffer saline solution and AgAuNPs (70 μL). Control parallels consisted of LB medium, inoculum (30 μL, OD_{600} = 0.8), and phosphate buffer saline solution. The experiment was performed in 8 parallels and 3 independent repetitions. The microtiter plate was covered with a lid and incubated at 37 °C and 150 rpm for 24 hours.

MTT assay

To measure the metabolic activity of the biofilm, a 3-(4,5-dimethylthiazol-2-yl)-2,5-diphenyltetrazolium bromide (MTT) reduction assay was conducted, following the method of Sabaeifard *et al.*[16] The wells were washed with saline and then treated with glucose solution (60 μL, 57.4 mg mL^{-1}) and MTT solution (50 μL, 1 mg mL^{-1}). The microtiter plate was covered and incubated in the dark at 37 °C and 150 rpm for 1 hour. After incubation, wash solution (100 μL) was added to each well, and the plate was agitated for 30 minutes at room temperature. The

wash solution comprised a mixture of dimethylformamide, phosphate buffer saline solution, acetic acid, and sodium dodecyl sulfate. Following the agitation, the color intensity was measured at 570 nm using a microtiter plate spectrophotometric reader (Sunrise reader, Tecan, Switzerland). The experiment was performed in eight parallels. The minimal biofilm inhibitory concentration ($MBIC_{50}$ and $MBIC_{90}$) was determined as the lowest concentration of the nanoparticle suspension that inhibited biofilm formation by 50% and 90%, respectively, compared to the control.[17] The MBIC assessment involved three independent replicates, all exhibiting consistent results within the range of studied concentrations.

Results and discussion

Nanoparticle characterization

Using extracts from waste of *Vitis vinifera* and *Cannabis sativa*, bimetallic nanoparticles were successfully prepared, with their formation monitored initially by the change in visible light absorbance, followed by analytical confirmation by UV-vis spectrophotometry. In the spectra, absorbances at wavelengths of 550 nm (*Vitis vinifera*) and 520 nm (*C. sativa*) are evident, which are caused by the plasmon resonance of the formed nanoparticles (see Fig. 2). In the study by Abbasi *et al.* (2018), the synthesis of AgAuNPs using an extract from *Cannabis sativa* leaves was investigated, with the absorption maximum observed at a wavelength of 538 nm.[18] Another study synthesized silver, gold, and bimetallic nanoparticles using an extract from *Dovyalis caffra* fruits. Absorption peaks were found at wavelengths of 430 nm (silver), 532 nm (gold), and 540 nm (bimetallic).[19] The synthesis of AgAuNPs was also achieved using an extract from *Stigmaphyllon ovatum* leaves, and a time-dependent experiment showed a shift in the absorption maximum from 534 nm after 30 minutes to 542 nm after 45 minutes.[20] Regarding the structure of bimetallic nanoparticles, literature suggests that the presence of a single absorption peak indicates an alloy nature.[21] The absorbance of 550 nm (*V. vinifera*) and 520 nm (*C. sativa*) observed in our work therefore corresponds to the range in which gold–silver alloy nanoparticles are found. The difference between nanoparticles synthesized by respective plant extract can be attributed to the difference in their size and shape profile (as demonstrated by TEM analysis, see below) which is a direct result of differences in composition of extracts from various plants.

The metal concentrations in the synthesized dispersion of AgAuNPs prepared using *Vitis vinifera* extract were determined by AAS to be 215.6 mg L^{-1} of silver and 393.3 mg L^{-1} of gold, while the concentrations of the synthesized dispersion of AgAuNPs prepared using *Cannabis sativa* extract were determined by AAS to be 106.4 mg L^{-1} of silver and 179.0 mg L^{-1} of gold. Specific descriptions of methods for determining the concentration of metal nanoparticles are relatively scarce in the literature. A large portion of experimental studies does not address the determination of nanoparticle concentration at all, and the input concentration of the precursor metal is often used as the concentration for subsequent experiments (*e.g.*, antimicrobial activity tests). This assumes 100% conversion of metal ions without knowledge of the synthesis process mechanism or the actual yield of nanoparticle production.[22] However, there are some studies that focus on determining the actual concentration of nanoparticle dispersions. In a study investigating the production of gold and silver nanoparticles using an extract from *Cannabis sativa*, the concentration was determined using inductively coupled plasma mass spectrometry (ICP-MS). Through analysis of individual particles, it was found that the number of nanoparticles per milliliter ranged from 26 to 83 billion. When converted to mass concentration, the concentrations ranged from 0.7 to 4.5 mg mL^{-1}.[23] In a study on the synthesis of copper nanoparticles using an extract from *Magnolia kobus* leaves, a linear relationship was found between the nanoparticle concentration measured by ICP-MS and the size of the absorption peak caused by surface plasmon resonance.[24] A special subtype of ICP-MS (single particle ICP-MS or spICP-MS) is an emerging methodological trend, where concentration, composition and size of nanoparticles can be analysed on single particle-level and then statistically evaluated.[25–27]

The basic morphology of AgAuNPs created using *Vitis vinifera* extract was explored using transmission electron microscopy,

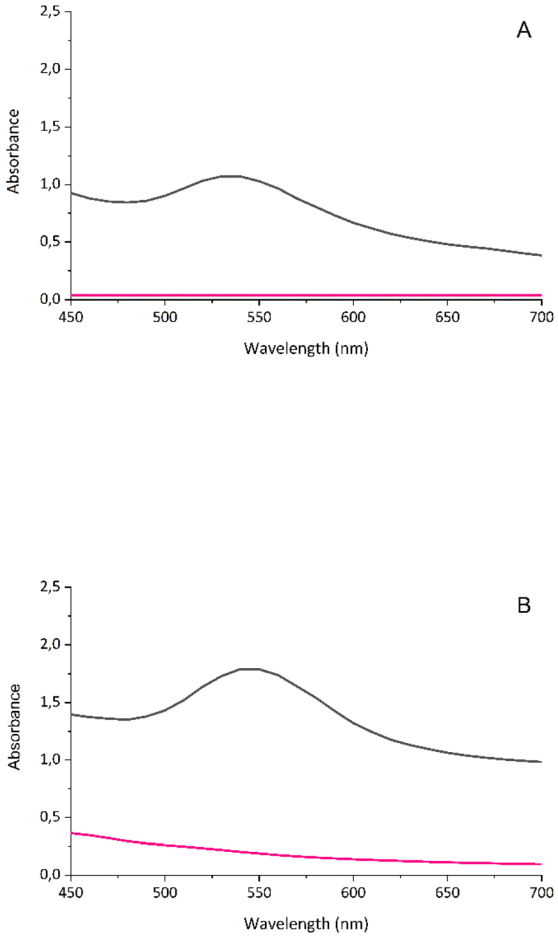

Fig. 2 UV-vis absorption spectra of AgAuNPs prepared using *Vitis vinifera* (A) or *Cannabis sativa* (B) waste extract; ■ – AgAuNPs, ■ – plant extract. The data show a distinctive peak at wavelengths characteristic for bimetallic alloy nanoparticles between 500 and 550 nm.

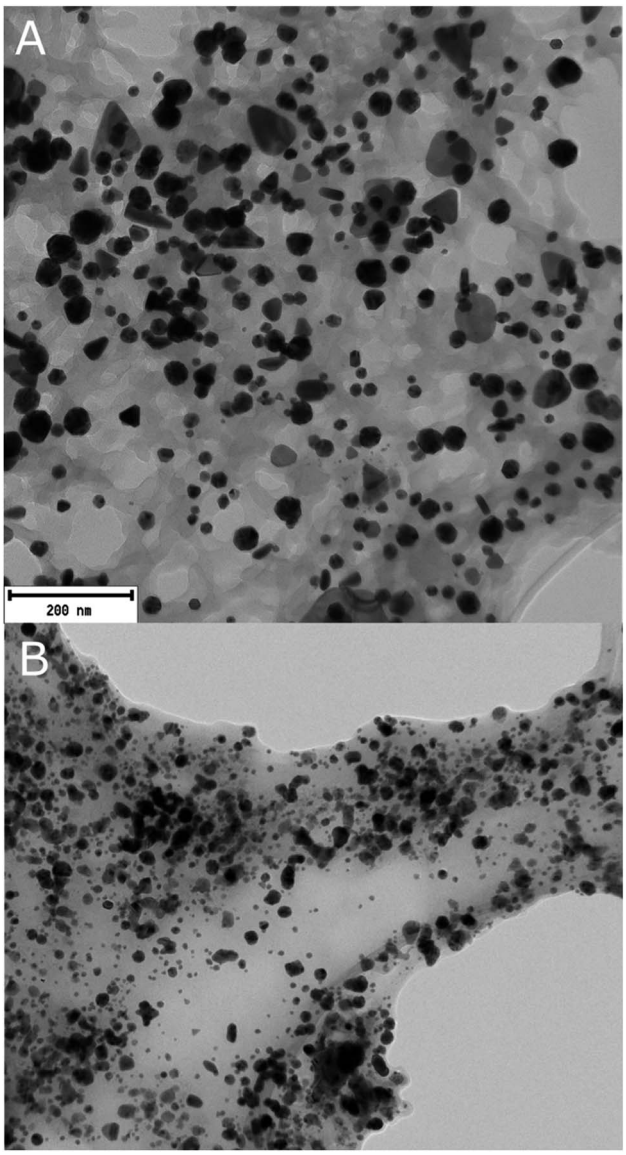

Fig. 3 Transmission Electron Microscopy (TEM) Images of AgAuNPs synthesized using plant extracts. This figure presents TEM images of AgAuNPs produced using two different plant extracts. Panel (A) shows nanoparticles synthesized using *Vitis vinifera* extract, exhibiting a variety of shapes. Panel (B) displays nanoparticles synthesized using *Cannabis sativa* extract, predominantly showing spherical shapes. The images provide a visual representation of the nanoparticle morphologies. TEM revealed diverse morphologies of bimetallic nanoparticles synthesized with *Vitis vinifera* extract, including spherical, rod-shaped, triangular, polygonal, and ellipsoidal particles. Bimetallic nanoparticles synthesized using *Cannabis sativa* extract exhibit predominantly spherical shapes, with occasional polygonal or triangular particles.

revealing high heterogeneity with nanoparticles exhibiting spherical, rod-like, triangular, polygonal, and ellipsoidal shapes. Similarly, the basic morphology of AgAuNPs, created using *Cannabis sativa* extract was investigated, showing predominantly spherical nanoparticles with occasional polygonal or triangular shapes (see Fig. 3). TEM photographs were utilized for image analysis, resulting in size histograms of the produced nanoparticles. For nanoparticles created using *Vitis vinifera* extract, the particle size ranged from 6 to 94 nanometers, with the highest frequency (42%) observed between 14 and 23 nm. Similarly, for nanoparticles created using *Cannabis sativa* extract, the majority (63%) of the produced nanoparticles fell within the size range of 1–7 nm, while the largest synthesized nanoparticles had an average diameter of 26–29 nm (1%) (see Fig. 4). In terms of size, a study utilizing an extract from *Triticum aestivum* observed nanoparticles with diameters ranging from 5 to 40 nm. In other studies using fungal xylanase or an extract from *Lawsonia inermis* seeds, nanoparticles with sizes ranging from 10 to 52 nm were observed.[28–30] Therefore, the AgAuNPs (*V. vinifera*) in our work showed the highest variability in size when compared with literature, while AgAuNPs (*C. sativa*) synthesized in our work displayed unusually small size which, according to literature, may lead to higher antimicrobial properties.

X-ray photoelectron spectroscopy (XPS) of bimetallic nanoparticles produced using *Vitis vinifera* extract revealed the presence of carbon, oxygen, silver, and gold on their surface layers, with relative compositions of 35.7%, 46.9%, 4.9%, and 12.5%, respectively, and 33.3%, 29.1%, 23.5%, and 14.1%, respectively for bimetallic nanoparticles produced using *Cannabis sativa* extract. In the case of bimetallic nanoparticles, a study utilizing an extract from *Diopyros kaki* leaves confirmed

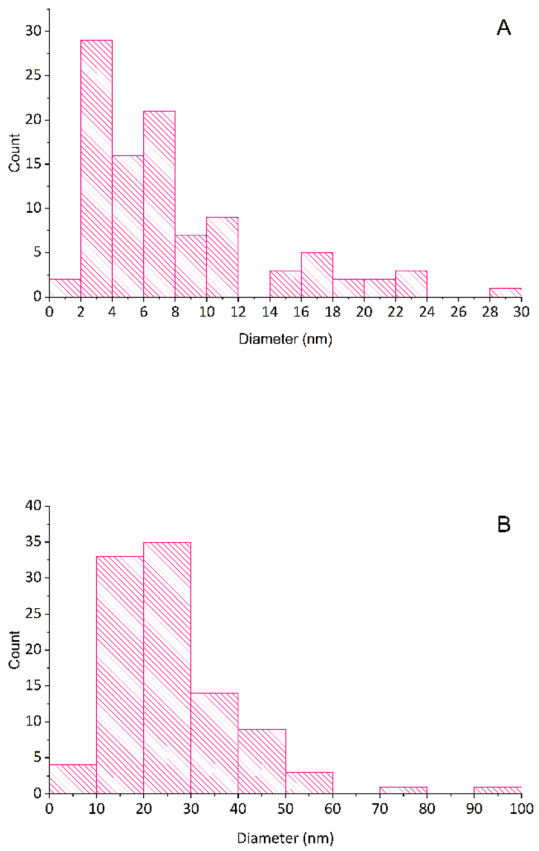

Fig. 4 Histogram representing the size distribution of bimetallic nanoparticles, in nanometers (nm), synthesized using an extract derived from *Vitis vinifera* (A) or *Cannabis sativa* (B) waste, where most nanoparticles exhibited sizes between 6 and 58 nm or 1 to 12 nm, respectively.

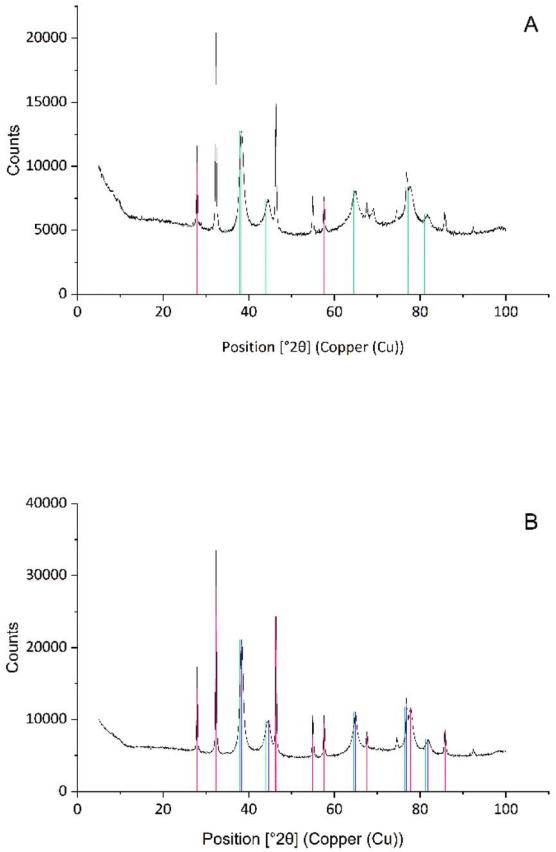

Fig. 5 XRD spectrum of bimetallic nanoparticles synthesized using *Vitis vinifera* (A) or *Cannabis sativa* (B) waste extract. The *x*-axis represents the diffraction angles (2θ), while the *y*-axis denotes the intensity of the diffracted X-rays. The diffractograms confirmed the presence of metallic silver, gold and chlorargyrite in both tested samples.

the presence of gold and silver through peaks at 83.9 and 87.6; 367.7 and 373.7 eV, respectively, in the X-ray photoelectron spectroscopy spectra.[31,32] In a study where an extract from *Antigonon leptopus* leaves was used for the synthesis of bimetallic nanoparticles, in addition to gold and silver, carbon, oxygen, and nitrogen were also identified through peaks at 284.8; 532.7; and 399.9 eV, respectively.[33] Consistent with the literature, this work identified the presence of gold, silver, carbon, and oxygen through peaks at 83.8; 373.8; 284.6; and 532.6 eV for the *Vitis vinifera* extract, and 84.4; 368.0; 285.2; and 532.4 eV for the *Cannabis sativa* extract.

X-ray diffractograms of bimetallic nanoparticles synthesized using *Cannabis sativa* extract exhibited diffraction peaks at 2θ = 38.3°, 44.5°, 64.7°, and 77.7°, corresponding to the indexing of (1 1 1), (2 0 0), (2 2 0), and (3 1 1) planes of metallic gold. Additionally, diffraction peaks at 2θ = 38.2°, 44.3°, 64.6°, and 77.4° can be indexed to (1 1 1), (2 0 0), (2 2 0), (3 1 1), and (2 2 2) planes of metallic silver, while peaks at 2θ = 27.9°, 32.3°, 46.3°, 54.9°, 57.5°, 67.6°, and 76.8° can be attributed to (1 1 1), (2 0 0), (2 2 0), (3 3 1), (2 2 2), (4 0 0), and (4 2 0) planes of silver chloride (see Fig. 5). The X-ray diffraction data of bimetallic nanoparticles synthesized using *Vitis vinifera* extract display diffraction peaks at 2θ = 38.3°, 44.5°, 64.7°, and 77.7°, corresponding to the indexing of (1 1 1), (2 0 0), (2 2 0), and (3 1 1) planes of metallic gold. Additionally, diffraction peaks at 2θ = 38.2°, 44.3°, 64.6°, and 77.4° can be indexed to (1 1 1), (2 0 0), (2 2 0), (3 1 1), and (2 2 2) planes of metallic silver, while peaks at 2θ = 27.9°, 32.3°, 46.3°, 54.9°, 57.5°, 67.6°, and 76.8° can be attributed to (1 1 1), (2 0 0), (2 2 0), (3 3 1), (2 2 2), (4 0 0), and (4 2 0) planes of silver chloride (see Fig. 5). The crystallographic analysis of bimetallic nanoparticles synthesized using an extract from *Dovyalis caffra* identified peaks at 2θ values of 38.1, 44.3, 64.5, and 77.5° corresponding to the planes (1 1 1), (2 0 0), (2 2 0), and (3 1 1) of the face-centered cubic lattice of gold. Additionally, peaks at 2θ values of 38.1, 64.4, and 76.5° were observed, corresponding to the planes (1 1 1), (2 2 0), and (3 1 1) of the face-centered cubic lattice of silver. Furthermore, peaks at 2θ values of 32.0 and 46.0° were observed, corresponding to the planes (2 0 0) and (2 2 0) of silver chloride. Similar results, except for the presence of silver chloride, were obtained in studies investigating the preparation of bimetallic nanoparticles using extracts from *Moringa oleifera* and *Piper betle*.[19,34,35] The X-ray diffractograms of bimetallic nanoparticles synthesized using *Cannabis sativa*, *Vitis vinifera*, and *Dovyalis caffra* extracts show similar diffraction peaks corresponding to the planes of metallic gold and silver. However, the nanoparticles synthesized using *Dovyalis caffra* extract exhibited a unique pattern with the absence of certain peaks corresponding to silver chloride, a characteristic also observed in nanoparticles synthesized using *Moringa oleifera* and *Piper betle* extracts. This suggests a potential influence of the extract type on the formation and composition of the bimetallic nanoparticles. Both AgAuNPs in this study exhibit characteristics indicative of a solid-solute type structure, as opposed to being intermetallic. This structural formation can be hypothesized to be influenced by the role of strong d-orbital interactions and anisotropic ordering in bimetallic nanoparticle synthesis. Additionally, the thermal and kinetic conditions during synthesis, such as temperature and reduction rates, significantly influence the alloying process and final structure. Our experimental conditions, particularly the unique properties of the plant extracts used, may have favored the formation of a solid solute structure by altering these synthesis dynamics.[36–38]

Fourier-transform infrared spectroscopy (FTIR) was used to identify functional groups present on the surface of bimetallic nanoparticles synthesized using *Vitis vinifera* extract (see Fig. 6). The broad absorption band at 3373 cm^{-1} indicates the presence of O–H groups, aromatic compounds, or C=C double bonds. The combined valence vibrations at 1609 and 1107 cm^{-1} confirm the presence of these C=C groups. Additional absorption bands at 1609 and 1512 cm^{-1} confirm the presence of proteins. The width of the right shoulder of the absorption band at 3373 cm^{-1}, along with valence vibrations at 1609 and 1512 cm^{-1}, suggests the presence of aromatic compounds. Deformation vibrations at 820 cm^{-1} indicate substitution of these aromatic compounds in the para position. Deformation vibrations at 1445 and 1107 cm^{-1} are associated with the presence of C–H and C–O groups, specifically indicating the

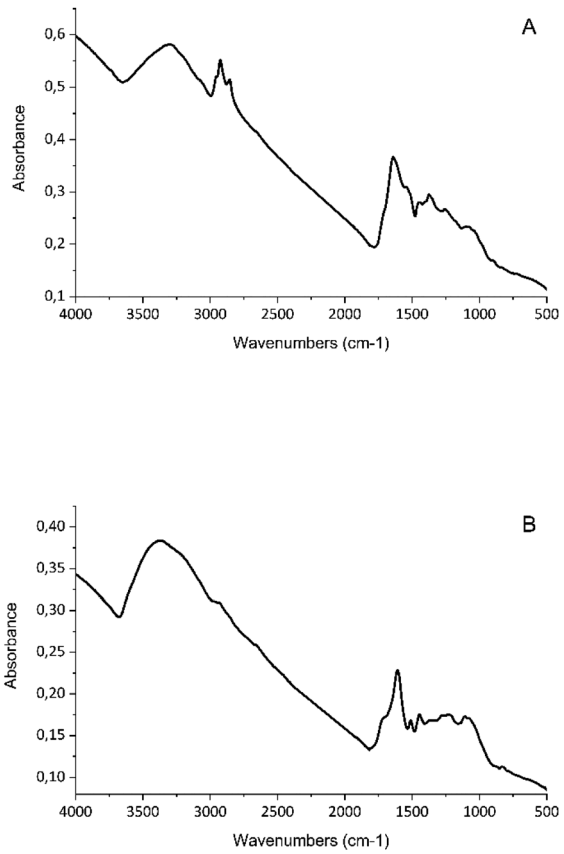

Fig. 6 Fourier Transform Infrared (FTIR) spectrum of bimetallic nanoparticles. This figure displays the FTIR spectrum of bimetallic nanoparticles synthesized using *Vitis vinifera* (A) or *Cannabis sativa* (B) waste extract. The *x*-axis represents the wavenumber (in cm^{-1}), and the *y*-axis denotes the absorbance. Each peak in the spectrum corresponds to a specific vibrational mode of a functional group present in the nanoparticles. FTIR spectroscopy reveals functional groups on the surfaces of bimetallic nanoparticles synthesized using *Vitis vinifera* and *Cannabis sativa* extracts. Peaks at specific wavenumbers confirm the presence of various functional groups, including C=C bonds, O–H groups, and C–O bonds, as well as valence vibrations of C–H bonds.

presence of alcohols, ethers, carboxylic groups, or esters. For AgAuNPs synthesized using *Cannabis sativa* extract (see Fig. 6), the absorption band at 3306 cm^{-1} suggests the presence of O–H bonds. The combination with valence vibrations at 1640 cm^{-1} confirms the presence of C=C bonds, and the absorption at 1550 and 1050 cm^{-1} indicates the valence vibration of C–O bonds. Valence vibrations of C–H bonds were observed at 2925 and 2855 cm^{-1}, along with deformation vibrations at 1450 and 1374 cm^{-1}. Absorption bands at 3306 and 2855 cm^{-1} confirm valence vibrations of primary and secondary amines, while bands at 3306 and 2925 cm^{-1} confirm valence vibrations of hydroxyl groups. Valence vibrations at 1640 cm^{-1} indicate the presence of carbonyl groups. The broad absorption band at 1050 cm^{-1} may signify valence vibrations of C–N bonds in aliphatic amines.

In studies investigating the dispersion of silver or gold nanoparticles synthesized using *Cannabis sativa* extract, absorption bands were detected at 3332 cm^{-1} indicating the presence of O–H groups, valence vibration bands at 1741 cm^{-1} or 1604 cm^{-1} indicating the presence of C=C bond, and an increased absorption band at 1019 cm^{-1} indicating the valence vibration of the C–O bond. In addition, clear absorption bands of valence vibrations of carbonyl groups, which may belong to proteins, were observed at 1635 cm^{-1}. Valence vibrations of C–N groups of amines were also observed at 1045 cm^{-1}. In this study, the presence of O–H groups was confirmed with an absorption band at 3305 cm^{-1}, and the presence of C=C bond was indicated by valence vibration band at 1641 cm^{-1}. Other identified groups included C–O bonds with absorption bands at 1536 cm^{-1} and 1050 cm^{-1}, and a broader absorption band of aliphatic amines at 1050 cm^{-1}. For silver nanoparticles and bimetallic nanoparticles synthesized in this study using *Cannabis sativa* extract, the presence of valence vibration of the C–Cl bond with absorption at 700 cm^{-1} was detected. Similar results were obtained in a study examining the synthesis of silver nanoparticles using *Cannabis sativa*, where peaks at 769 cm^{-1}, 687 cm^{-1}, and 526 cm^{-1} were attributed to these vibrations. The reducing and stabilizing properties were attributed to reducing sugars or proteins, while the purely reducing activity likely resulted from terpenoids and flavonoids.[23,39]

In the case of nanoparticles synthesized from *Vitis vinifera* extract, wide absorption bands were identified in the literature at 3421–3469 cm^{-1}, indicating the presence of O–H groups. In combination with the valence vibration at 1650 cm^{-1} characteristic of C=C bonds in the aromatic ring, the participation of phenolic compounds in nanoparticle synthesis can be considered. Additionally, a deformation vibration at 820 cm^{-1}, suggesting *para*-substitution, was identified in this study. Absorption bands in the range of 1315 cm^{-1} and 1730 cm^{-1} are characteristic of valence vibrations of C=O and C–O groups, indicating the presence of carboxylic acids (*e.g.*, gallic or apple acids). The involvement of proteins was confirmed in the literature through the identification of absorption peaks indicating the presence of amides at 1655 cm^{-1}, combined with the aforementioned C=O groups.[40–42] In this study, the presence of O–H groups was confirmed by a wide absorption band at 3326 cm^{-1}, which also provides an indication of the occurrence of aromatic compounds. These findings were further supported by the identification of valence vibrations of C=C groups at 1605 cm^{-1} and 1108 cm^{-1}. Our results also confirmed the participation of proteins in nanoparticle synthesis, as additional peaks were observed at 1605 cm^{-1} and 1514 cm^{-1}. Deformation vibrations at 1446 cm^{-1} and 1108 cm^{-1}, associated with the presence of C–H and C–O groups, were also observed, indicating the involvement of primary and secondary alcohols.

Antimicrobial properties

The evaluation of antibacterial properties involved assessing inhibitory activity against both planktonic and adherent cells, as well as the bactericidal activity of the synthesized nanoparticles (see Tables 1 and 2). Inhibition of adherent cells was determined by total biofilm biomass and metabolic activity assays. Studies investigating the inhibitory activity of metal

Table 1 Antimicrobial properties of bimetallic nanoparticles produced using *Vitis vinifera* waste extract

	Ag : Au (mg L^{-1})		
	MIC_{80}	MBC	$MBIC_{80}$
P. aeruginosa DBM 3081	6.8 : 12.3	10.1 : 18.5	13.9 : 25.3
P. aeruginosa DBM 3777	4.1 : 7.4	4.1 : 7.4	Not found
P. aeruginosa ATCC 10145	6.8 : 12.3	33.7 : 61.5	2.7 : 4.9
P. aeruginosa ATCC 15442	2.7 : 4.9	13.5 : 24.6	1.4 : 2.5
PAO1	4.1 : 7.4	Not found	6.9 : 12.6

Table 2 Antimicrobial properties of bimetallic nanoparticles produced using *Cannabis sativa* waste extract

	Ag : Au (mg L^{-1})		
	MIC_{80}	MBC	$MBIC_{80}$
P. aeruginosa DBM 3081	2.0 : 3.4	0.2 : 0.3	6.8 : 11.5
P. aeruginosa DBM 3777	2.0 : 3.4	10.0 : 16.8	6.8 : 11.5
P. aeruginosa ATCC 10145	2.0 : 3.4	0.7 : 1.1	6.8 : 11.5
P. aeruginosa ATCC 15442	1.3 : 2.2	1.3 : 2.2	13.3 : 22.4
PAO1	2.0 : 3.4	Not found	3.4 : 5.7

nanoparticles synthesized using "green" methods exhibit a large variability in terms of nanoparticle properties and tested microorganisms. Similarly, to the characterization of bio-synthesized nanoparticles mentioned above, a significant portion of studies lacks important information such as the specific strain of the tested microorganism, the concentration of nanoparticles used for testing, or the specific experimental setup. In terms of experimental design, the majority of studies employ methods like disk diffusion or well diffusion.[22] These aforementioned factors contribute to the considerable variation in the results presented in the studies and differences in the activity of the specific nanoparticles used.

Because bimetallic nanoparticles derive their antimicrobial effect from both gold and silver with their respective mechanisms of action, we decided to investigate the concentrations of both metals in the dispersion. We then assign the produced nanoparticles with dual concentration, which is reflected both in the text (by mentioning both metals' concentrations explicitly) and in tables and figures (by using "Ag : Au (mg mL^{-1})" format).

By studying the effects of bimetallic nanoparticles synthesized using *Vitis vinifera* extract on planktonic cells of *P. aeruginosa*, MIC_{80} values were found for all five strains, ranging from 2.7 to 6.8 mg L^{-1} of silver and 4.9 to 12.3 mg L^{-1} of gold. In investigating the inhibitory activity of bimetallic nanoparticles synthesized using *Cannabis sativa*, MIC_{80} values were found for all studied strains of *P. aeruginosa*. The concentration range in which this inhibitory activity was observed was 1.3 to 2 mg L^{-1} of silver and 2.2 to 3.4 mg L^{-1} of gold.

Bactericidal activity of bimetallic nanoparticles synthesized using *Vitis vinifera* extract was observed in all studied strains of *P. aeruginosa* except PAO1, with MBC ranging from 4.1 to 33.7 mg L^{-1} of silver and 7.4 to 61.5 mg L^{-1} of gold. Bimetallic nanoparticles synthesized using *Cannabis sativa* extract exhibited bactericidal activity against all studied strains of *P. aeruginosa* except PAO1. MBC values were found across a wide concentration range, specifically 0.2 to 10 mg L^{-1} of silver and 0.3 to 16.8 mg L^{-1} of gold.

Table 3 Minimal bactericidal concentration to minimal inhibitory concentration ratio of bimetallic nanoparticles produced using *Vitis vinifera* and *Cannabis sativa* waste extracts

	MBC : MIC ratio (type of effect)	
	Vitis vinifera	*Cannabis sativa*
P. aeruginosa DBM 3081	1.5 (bactericidal)	0.1 (bactericidal)
P. aeruginosa DBM 3777	1.0 (bactericidal)	5.0 (bacteriostatic)
P. aeruginosa ATCC 10145	5.0 (bacteriostatic)	0.4 (bactericidal)
P. aeruginosa ATCC 15442	3.2 (bactericidal)	1.0 (bactericidal)
PAO1	Not found	Not found

According to a typology proposed by Ayala-Núñez *et al.*, if the ratio of MBC to MIC is equal or smaller than 4 the effect is considered as bactericidal, but if the ratio of MBC to MIC is greater than 4 then the effect was defined as bacteriostatic.[43]

Both nanoparticles produced using *Vitis vinifera* and *Cannabis sativa* exhibited bactericidal activity against some strains (*e.g.*, DBM 3081 and ATCC 15442), while in some cases they have shown only bacteriostatic effect (see Table 3). PAO1 did not display any of these effects since MBC was not achieved in the concentration range used.

Bimetallic nanoparticles synthesized using *Vitis vinifera* extract demonstrated inhibitory activity against adhering cells of *P. aeruginosa* in all studied strains (see Fig. 7). The $MBIC_{80}$ values ranged from 1.4 to 13.9 mg L^{-1} of silver and 2.5 to 25.3 mg L^{-1} of gold. Inhibitory activity of bimetallic nanoparticles produced using *Cannabis sativa* extract against adhering cells of *P. aeruginosa* was also investigated. The $MBIC_{80}$ values were found in the concentration range of 3.4 to 13.3 mg L^{-1} of silver and 5.7 to 22.4 mg L^{-1} of gold. These results show a promising trend. While in antibiotics MBICs can be at least 500 higher than MICs, nanoparticles in this study effectively inhibited biofilm formation in concentrations only 3–10 times higher than MIC.

AgAuNPs produced using *Cannabis sativa* consistently exhibited strong inhibition against planktonic cells at lower concentrations. While the extract alone does not inhibit Gram negative bacteria, according to both our experiments (data not shown) and literature, it was effective in combination with other agents (*e.g.*, antibiotics).[44] Some potentiating effect of the combined action of AgAuNPs and *Cannabis sativa* extract could be possible.

Bimetallic alloy nanoparticles are relatively rare in the literature, and although some studies examining their antimicrobial effects can be found, this study is one of the few exploring a range of pharmacodynamic parameters of antimicrobial activity (MIC, MBC, MBIC).[45] When investigating the antibacterial effect of bimetallic nanoparticles produced using an extract from *Ziziphus spina-christi* leaves, the MIC was found to

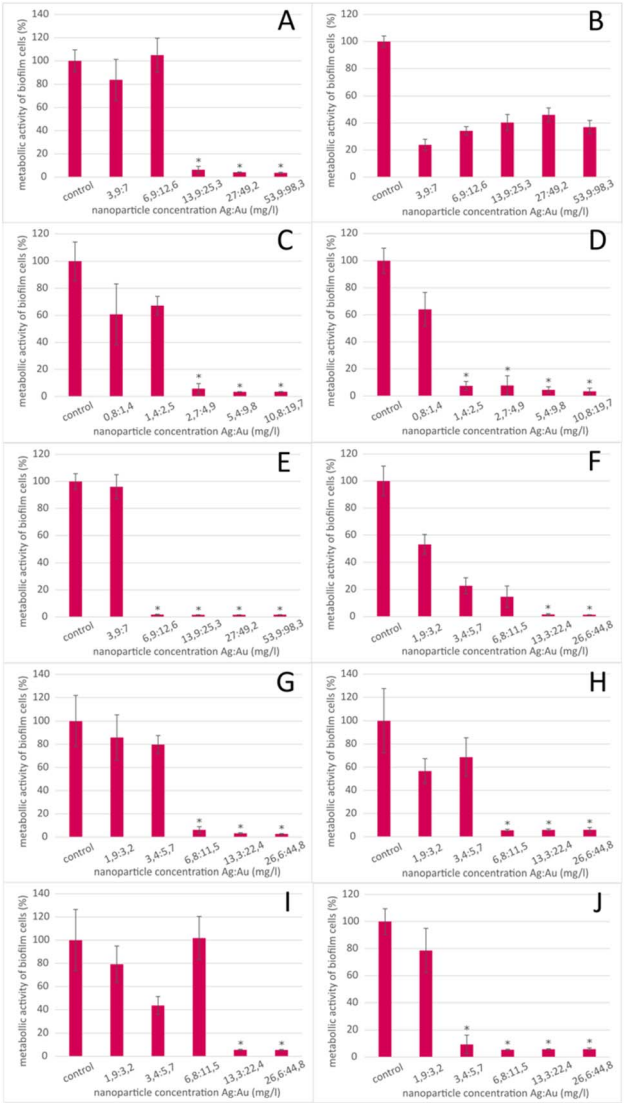

Fig. 7 Metabolic activity of *P. aeruginosa* in response to bimetallic nanoparticles. This figure presents the results of MBIC testing for *P. aeruginosa* (strains DBM 3081, DBM 3777, ATCC 10145, ATCC 15442 and PAO1) exposed to bimetallic nanoparticles synthesized using two different plant extracts. Graphs (A–E) show the metabolic activity of *P. aeruginosa* at different concentrations of nanoparticles produced using *Vitis vinifera* extract, with $MBIC_{80}$ values ranging from 1.4 to 13.9 mg L^{-1} of silver and 2.5 to 25.3 mg L^{-1} of gold. Graphs (F–J) display the metabolic activity at varying concentrations of nanoparticles synthesized using *Cannabis sativa* extract, where the $MBIC_{80}$ values were found in the concentration range of 3.4 to 13.3 mg L^{-1} of silver and 5.7 to 22.4 mg L^{-1} of gold. The graphs provide a visual representation of the inhibitory activity of these nanoparticles against both planktonic and adhering cells.

be 61 mg L^{-1}, and the MBC was 93.3 mg L^{-1}. In another study, where bimetallic nanoparticles were created using quercetin, the MIC and MBC values were determined as 5 and 10 mg L^{-1}, respectively.[46,47] AgAuNPs in our study exhibited strong antibacterial activity at relatively low range, even when compared to studies where silver nanoparticles were used.[48–50] These results show promise especially considering silver nanoparticles are characterized by higher toxicity for mammalian cells compared to gold nanoparticles. Therefore, it can be expected the toxicity of AgAuNPs in this study is lowered while the antibacterial activity is preserved.[51]

Regarding the comparison of AgAuNPs in our study, the enhanced antimicrobial activity of nanoparticles synthesized using *Cannabis sativa* extract compared to those from *Vitis vinifera* can be attributed to several distinct characteristics. Firstly, nanoparticles from *Cannabis sativa* exhibited smaller sizes (1–7 nm), increasing their surface area-to-volume ratio for more efficient microbial interaction. Secondly, surface chemistry analysis revealed different functional groups on these nanoparticles, influencing their interaction with the bacterial cell. Lastly, the synergy between metallic components and *Cannabis sativa* phytochemicals might enhance antimicrobial efficacy.[52–54] These factors collectively contribute to the superior inhibitory effect of nanoparticles produced with *Cannabis sativa*.

Conclusions

This study demonstrates the successful synthesis of bimetallic nanoparticles using waste extracts from *Vitis vinifera* and *Cannabis sativa*. These nanoparticles exhibited remarkable antimicrobial activity against *P. aeruginosa*, a common pathogen responsible for nosocomial infections and a major contributor to antibiotic resistance, while promising lower toxicity against mammalian cells than silver nanoparticles.

The utilization of agricultural waste for nanoparticle production presents a sustainable and cost-effective approach. The development of nanoparticle coatings derived from such waste sources holds great potential for combating nosocomial infections, addressing antibiotic resistance, and offering affordable solutions for infection control in healthcare settings. Further investigations should focus on optimizing the synthesis process and evaluating the nanoparticles' efficacy in real-world applications.

Conflicts of interest

There are no conflicts to declare.

Notes and references

1 S. K. Srikar, D. D. Giri, D. B. Pal, P. K. Mishra and S. N. Upadhyay, *Green Sustainable Chem.*, 2016, **06**, 34–56.
2 F. Chamorro, M. Carpena, M. Fraga-Corral, J. Echave, M. S. Riaz Rajoka, F. J. Barba, H. Cao, J. Xiao, M. A. Prieto and J. Simal-Gandara, *Food Chem.*, 2022, **370**, 131315.
3 Y. Bao, J. He, K. Song, J. Guo, X. Zhou and S. Liu, *J. Chem.*, 2021, **2021**, e6562687.
4 S. Iravani, *Green Chem.*, 2011, **13**, 2638–2650.
5 I. A. Adelere and A. Lateef, *Nanotechnol. Rev.*, 2016, **5**, 567–587.
6 N. Arora, K. Thangavelu and G. N. Karanikolos, *Front. Chem.*, 2020, **8**, 412.
7 H. T. Nasrabadi, E. Abbasi, S. Davaran, M. Kouhi and A. Akbarzadeh, *Artif. Cells, Nanomed., Biotechnol.*, 2016, **44**, 376–380.

8 O. T. Fanoro and O. S. Oluwafemi, *Pharmaceutics*, 2020, **12**, 1044.
9 K. Gopinath, S. Kumaraguru, K. Bhakyaraj, S. Mohan, K. S. Venkatesh, M. Esakkirajan, P. Kaleeswarran, N. S. Alharbi, S. Kadaikunnan, M. Govindarajan, G. Benelli and A. Arumugam, *Microb. Pathog.*, 2016, **101**, 1–11.
10 A. Miškovská, M. Rabochová, J. Michailidu, J. Masák, A. Čejková, J. Lorinčík and O. Mať átková, *PLoS One*, 2022, **17**, e0272844.
11 M. Rollová, L. Gharwalova, A. Krmela, V. Schulzová, J. Hajšlová, P. Jaroš, I. Kolouchová and O. Mať átková, *Czech J. Food Sci.*, 2020, **38**, 137–143.
12 A. A. AbdelHamid, M. A. Al-Ghobashy, M. Fawzy, M. B. Mohamed and M. M. S. A. Abdel-Mottaleb, *ACS Sustainable Chem. Eng.*, 2013, **1**, 1520–1529.
13 M. Sharma, R. Manoharlal, A. S. Negi and R. Prasad, *FEMS Yeast Res.*, 2010, **10**, 570–578.
14 E. Serra, L. A. Hidalgo-Bastida, J. Verran, D. Williams and S. Malic, *Pathogens*, 2018, **7**, 15.
15 J. J. Rahal and M. S. Simberkoff, *Antimicrob. Agents Chemother.*, 1979, **16**, 13–18.
16 P. Sabaeifard, A. Abdi-Ali, M. R. Soudi and R. Dinarvand, *J. Microbiol. Methods*, 2014, **105**, 134–140.
17 D.-S. Shin and Y.-B. Eom, *Can. J. Microbiol.*, 2019, **65**(10), 713–721.
18 B. H. Abbasi, M. Zaka, S. S. Hashmi and Z. Khan, *IET Nanobiotechnol.*, 2018, **12**, 277–284.
19 J. O. Adeyemi, E. E. Elemike, D. C. Onwudiwe and M. Singh, *Inorg. Chem. Commun.*, 2019, **109**, 107569.
20 E. E. Elemike, D. C. Onwudiwe, N. Nundkumar, M. Singh and O. Iyekowa, *Mater. Lett.*, 2019, **243**, 148–152.
21 M. Amina, N. M. Al Musayeib, N. A. Alarfaj, M. F. El-Tohamy and G. A. Al-Hamoud, *Nanomaterials*, 2020, **10**, 2453.
22 O. Mať átková, J. Michailidu, A. Miškovská, I. Kolouchová, J. Masák and A. Čejková, *Biotechnol. Adv.*, 2022, **58**, 107905.
23 P. Singh, S. Pandit, J. Garnæs, S. Tunjic, V. R. Mokkapati, A. Sultan, A. Thygesen, A. Mackevica, R. V. Mateiu, A. E. Daugaard, A. Baun and I. Mijakovic, *Int. J. Nanomed.*, 2018, **13**, 3571–3591.
24 H.-J. Lee, G. Lee, N. R. Jang, J. H. Yun, J. Y. Song and B. S. Kim, Technical Proceedings of the 2011 NSTI Nanotechnology Conference and Expo, *NSTI-Nanotech 2011*, 2011, vol. 1, pp. 371–374.
25 A. Filippi, A. Mattiello, R. Musetti, E. Petrussa, E. Braidot and L. Marchiol, *AIP Conf. Proc.*, 2017, **1873**, 020004.
26 D. Mozhayeva and C. Engelhard, *J. Anal. At. Spectrom.*, 2020, **35**, 1740–1783.
27 S. Rana, S. Kapoor, S. Sharma and A. Kalia, *Food Sci. Biotechnol.*, 2023, **32**, 2079–2092.
28 B. Akilandaeaswari and K. Muthu, *J. Taiwan Inst. Chem. Eng.*, 2021, **127**, 292–301.
29 J. A. Elegbede, A. Lateef, M. A. Azeez, T. B. Asafa, T. A. Yekeen, I. C. Oladipo, A. S. Hakeem, L. S. Beukes and E. B. Gueguim-Kana, *Biotechnol. Prog.*, 2019, **35**, e2829.
30 V. Pahal, P. Kumar, P. Kumar and V. Kumar, *Plant Sci. Today*, 2022, **9**, 345–356.
31 J. Y. Song and B. S. Kim, *Korean J. Chem. Eng.*, 2008, **25**, 808–811.
32 Y. Weng, J. Li, X. Ding, B. Wang, S. Dai, Y. Zhou, R. Pang, Y. Zhao, H. Xu, B. Tian and Y. Hua, *Int. J. Nanomed.*, 2020, **15**, 1823–1835.
33 S. U. Ganaie, T. Abbasi and S. A. Abbasi, *J. Exp. Nanosci.*, 2016, **11**, 395–417.
34 S. Gupta, H. Hemlata and K. K. Tejavath, Synthesis, characterization and comparative anticancer potential of photosynthesized mono and bimetallic nanoparticles using *Moringa oleifera* aqueous leaf extract, *Nano*, 2022, **17**(06), 2250047.
35 A. Lagashetty, S. K. Ganiger and Shashidhar, *Heliyon*, 2019, **5**, e02794.
36 J. Li and S. Sun, *Acc. Chem. Res.*, 2019, **52**, 2015–2025.
37 X. Wang, L. Altmann, J. Stöver, V. Zielasek, M. Bäumer, K. Al-Shamery, H. Borchert, J. Parisi and J. Kolny-Olesiak, *Chem. Mater.*, 2013, **25**, 1400–1407.
38 K. Loza, M. Heggen and M. Epple, *Adv. Funct. Mater.*, 2020, **30**, 1909260.
39 T. Singh, K. Jyoti, A. Patnaik, A. Singh and S. C. Chauhan, *Alexandria Eng. J.*, 2018, **57**, 3043–3051.
40 D. D. Gultekin, H. Nadaroglu, A. A. Gungor and N. H. Kishali, *Int. J. Second. Metab.*, 2017, **4**, 77–84.
41 M. Khalil, *Prog. Nanotechnol. Nanomater.*, 2014, **3**, 1–12.
42 S. Venkateswarlu, B. N. Kumar, B. Prathima, K. Anitha and N. V. V. Jyothi, *Phys. B*, 2015, **457**, 30–35.
43 N. V. Ayala-Núñez, H. H. Lara Villegas, L. del Carmen Ixtepan Turrent and C. Rodríguez Padilla, *Nanobiotechnol*, 2009, **5**, 2–9.
44 L. Schofs, M. D. Sparo and S. F. Sánchez Bruni, *Pharmacol. Res. Perspect.*, 2021, **9**, e00761.
45 M. D. Macia, E. Rojo-Molinero and A. Oliver, *Clin. Microbiol. Infect.*, 2014, **20**, 981–990.
46 S. Alzahrani, H. M. Ali, E. H. Althubaiti and M. M. Ahmed, *Indian J. Pharm. Sci.*, 2022, 42–53.
47 E. Bhatia and R. Banerjee, *J. Mater. Chem. B*, 2020, **8**, 4890–4898.
48 S. G. Ali, M. A. Ansari, H. M. Khan, M. Jalal, A. A. Mahdi and S. S. Cameotra, *J. Bionanosci.*, 2018, **8**, 544–553.
49 S. Arokiyaraj, S. Vincent, M. Saravanan, Y. Lee, Y. K. Oh and K. H. Kim, *Artif. Cells, Nanomed., Biotechnol.*, 2017, **45**, 372–379.
50 S. Feizi, E. Taghipour, P. Ghadam and P. Mohammadi, *Microb. Pathog.*, 2018, **125**, 33–42.
51 P. N. H. Diem, T. N. M. Phuong, N. Q. Hien, D. T. Quang, T. T. Hoa and N. D. Cuong, *J. Nanomater.*, 2020, **2020**, e7195048.
52 M. Khalaj, M. Kamali, M. E. V. Costa and I. Capela, *J. Cleaner Prod.*, 2020, **267**, 122036.
53 R. Vishwanath and B. Negi, *Curr. Res. Green Sustainable Chem.*, 2021, **4**, 100205.
54 S. Kumar, I. B. Basumatary, H. P. K. Sudhani, V. K. Bajpai, L. Chen, S. Shukla and A. Mukherjee, *Trends Food Sci. Technol.*, 2021, **112**, 651–666.